Pull-in/out analysis of nano/microelectromechanical switches with defective oxide layers

Yang Xu and N. R. Aluru

Citation: Appl. Phys. Lett. **95**, 073112 (2009); doi: 10.1063/1.3211111
View online: http://dx.doi.org/10.1063/1.3211111
View Table of Contents: http://apl.aip.org/resource/1/APPLAB/v95/i7
Published by the American Institute of Physics.

Pull-in/out analysis of nano/microelectromechanical switches with defective oxide layers

Yang Xu and N. R. Aluru[a)]
Beckman Institute for Advanced Science and Technology, University of Illinois at Urbana-Champaign, Urbana, Illinois 61801, USA

(Received 17 April 2009; accepted 28 July 2009; published online 21 August 2009)

We investigate the effect of surface and interior defects such as vacancies and broken bonds on the performance of nano/microelectromechanical (N/MEMS) switches. By combining multiscale electrostatic analysis with mechanical analysis, we compute the capacitance-voltage and pull-in/out voltages of N/MEMS switches in the presence of defects in the dielectric oxide layer. Our results indicate that both surface and interior defects can change the pull-in/out voltages leading to significant voltage offsets. These voltage offsets can lead to an eventual failure of the N/MEMS switch. © *2009 American Institute of Physics*. [DOI: 10.1063/1.3211111]

One of the popular applications of nano/microelectromechanical systems (N/MEMS) is rf switches, which are required to operate at high frequencies for millions of cycles.[1] During each cycle of operation, the moving electrode makes a mechanical contact with the thin dielectric (e.g., the oxide layer) and this can generate defects on the surface and inside the dielectric. The presence of these defects can lead to charge-trapping phenomena, which can significantly degrade the capacitive rf N/MEMS switch performance by altering the pull-in and pull-out voltages and eventually cause the switch to malfunction.[2–4] In addition to the defects that can be generated by repeated mechanical contacts, intrinsic defects (defects that are originally present) in oxide layers can significantly affect the reliability of rf-MEMS switches. Advances in nanotechnology have led to the fabrication of switches and resonators with the characteristic length scale of tens of nanometers.[5,6] The influence of defects in dielectric layers on capacitive NEMS switches can be quite significant. In this paper, using atomistic models based on tight-binding (TB) theory, we develop an understanding of how defects in oxide layers—in particular, oxygen vacancies and broken bonds—influence the pull-in and pull-out voltages of N/MEMS capacitive switches.

A simplified capacitive NEMS switch model, as shown in Fig. 1, is considered to investigate the influence of defects on the switch behavior. The switch consists of a moveable electrode (denoted as top electrode and assumed to be metallic) attached to a spring and the top electrode is separated from the dielectric oxide layer and the ground silicon substrate by a small air gap. To compute the static electromechanical behavior, a physical model where the continuum elastic theory (advanced theories based on multiscale methods can also be considered[7]) is coupled with the multiscale electrostatic theory is considered. The governing equations for electrostatic analysis are given by

$$\nabla^2\phi(\mathbf{x}) = \begin{cases} -\dfrac{\rho(\mathbf{x})}{\epsilon_{\mathrm{Si}}} & \text{in Si substrate,} \\ -\dfrac{e}{\epsilon_{\mathrm{ox}}}\dfrac{q(\mathbf{x})}{V_{\mathrm{SiO_2}}} & \text{in oxide,} \\ 0 & \text{in air,} \end{cases} \tag{1}$$

where $\rho(\mathbf{x})$ is the charge density in silicon substrate, $q(\mathbf{x})$ is the atomic charge due to the defective states, which can be computed by solving the TB equations as described below, $V_{\mathrm{SiO_2}}$ is the effective volume occupied by an atom in the oxide, e is the elementary charge, and ϵ_{Si} and ϵ_{ox} are the permittivity of Si and oxide, respectively. In the exterior domain, the Laplace equation is satisfied as shown in Eq. (1). The top electrode is assumed to be an equipotential surface. The oxide-air interface boundary condition is given by $\epsilon_{\mathrm{ox}}[\partial\phi(\mathbf{x})/\partial\mathbf{n}]|_{\mathrm{ox}} + \epsilon_{\mathrm{air}}[\partial\phi(\mathbf{x})/\partial\mathbf{n}]|_{\mathrm{air}} = \sigma_s$, where $[\partial\phi(\mathbf{x})/\partial\mathbf{n}]|_{\mathrm{air}}$ and $[\partial\phi(\mathbf{x})/\partial\mathbf{n}]|_{\mathrm{ox}}$ are the normal derivatives of the potential from the air and the oxide regions, respectively, ϵ_{air} is the permittivity of air, and σ_s is the charge density on the exposed surface of the oxide. The potential $\phi(\mathbf{x})$, the normal derivatives of the potential $\partial\phi(\mathbf{x})/\partial\mathbf{n}$, the surface charge density on the top electrode, $\sigma_t = -\epsilon_{\mathrm{air}}[\partial\phi(\mathbf{x})/\partial\mathbf{n}]|_{\mathrm{air}}$, and the charge density $\rho(\mathbf{x})$ are obtained by solving Eq. (1) self-consistently as described in

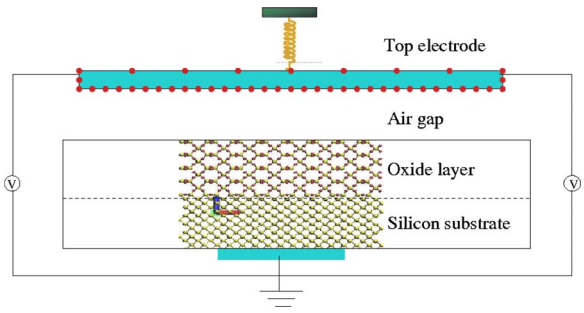

FIG. 1. (Color online) Schematic representation of a N/MEMS capactive switch. Defective states in oxide can play an important role on the pull-in/out behavior of N/MEMS switches. The oxide thickness d_{ox} is 5.83 nm, and the initial air gap g_0 is 6.0 nm. The silicon domain is *P*-type doped with $N_a = 9\times10^{17}$ cm^{-3}. The top silicon electrode has a geometry of $8\times100\times40$ nm^3 and the spring constant k is 43.26 N/m. The density of defects N_{defects} is varied from 1.8×10^{12} to 7.2×10^{12} cm^{-2}.

[a)]Author to whom correspondence should be addressed. Electronic mail: aluru@illinois.edu. URL: http://www.illinois.edu/aluru.

Ref. 8. The electrostatic force acting on the top electrode, f_{elec}, is then computed by the expression, $f_{\text{elec}} = W\int_0^L [\sigma_t^2(\mathbf{x})/2\epsilon_{\text{air}}]d\mathbf{x}$, where L is the length of the top electrode and W is the width into the plane. The restoring elastic force of the top electrode is computed by the expression $f_{\text{mech}} = -k(\mathbf{x}-\mathbf{x}_0)$, where $\mathbf{x}_0$ is the initial position of the top electrode.

The oxide layer is represented by crystalline Si/β-quartz SiO_2 atomistic structure and the positions of the atoms are adopted from Ref. 9. Oxide layers with nanometer dimensions can typically be modeled by the TB method. However, oxides with larger dimensions can contain bulklike subdomains, quantum confinement regions, and defect areas, and the use of any single-scale electrostatic physical theory to model the entire N/MEMS structure can either be inaccurate or computationally infeasible. For electrostatic analysis of the entire N/MEMS structure with reasonable accuracy and efficiency, a multiscale method, seamlessly combining, semiclassical, effective-mass Schrödinger, and TB theories, is used. The details of the method are presented in Ref. 8. To simulate localized defects in the oxide layer, a self-consistent sp^3 TB model is employed to calculate the electrostatic potential and the charge distribution. The TB parameters for silicon and oxygen atoms are taken from Ref. 9. By using α (β) to denote orbitals and i (j) to denote atoms, (atoms can be Si or O), the TB Hamiltonian element is given by

$$H_{i\alpha,j\beta} = \begin{cases} [\epsilon_{i\alpha} + e\phi(\mathbf{r}_i)] & \text{when } i=j \text{ and } \alpha=\beta, \\ H^0_{\alpha\beta}(r_{ij}) & \text{when } i \text{ and } j \text{ are neighbors}, \\ 0 & \text{otherwise}, \end{cases} \tag{2}$$

where $H^0_{\alpha\beta}(r_{ij})$ are directly obtained from the Slater and Koster's table,[10] $\epsilon_{i\alpha}$ is the onsite energy of the α orbital, $\phi(\mathbf{r}_i)$ is the electrostatic potential obtained by solving Eqs. (1) and (2) in the multiscale model.[8] In the self-consistent approach, an initial potential obtained by solving the semiclassical theory is used to compute the total TB Hamiltonian from Eq. (2). The local density of states (LDOS) of the α orbital of atom $\mathbf{r}_j$, which is a function of energy E, denoted by $N(\mathbf{r}_j, \alpha, E)$, are then obtained from the TB Hamiltonian,[8,11,12] and the atomic charge on atom j, $q(\mathbf{r}_j)$, is obtained from LDOS by the expression

$$q(\mathbf{r}_j) = -\left[\sum_{\alpha}\int_{-\infty}^{\infty} N(\mathbf{r}_j,\alpha,E)f_e(E)dE - Z_c\right], \tag{3}$$

where if atom j is a silicon or oxygen atom, the ionic core charge is Z_c=4.0. $f_e(E)$ is the Fermi–Dirac distribution for electrons. *Ab initio* calculations[13,14] and experiments[15,16] have presented the physical processes by which holes or electrons are captured by the defects in the oxide. Due to the limitation of the TB method, we can only simulate the charge distribution after the holes or electrons are captured by the defects. For defective states in the TB simulation, because each local oxide defect is an isolated system, the local Fermi energy is obtained using the law of total charge conservation.[17] That is, the summation of atomic charges near an isolated defect center is equal to the number of electrons/holes trapped by the defect. After the charge distribution is obtained, the potential is updated by using the new charge distribution and the process is repeated until a self-consistent solution is obtained.

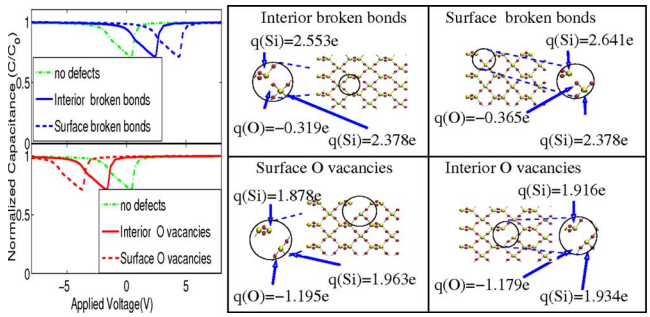

FIG. 2. (Color online) *C-V* characteristics of the structure when the top electrode and the gap between the top electrode and the oxide is fixed. The capacitance is normalized by the structure capacitance C_0, where $1/C_0 = g_0/\epsilon_{\text{air}} + d_{\text{ox}}/\epsilon_{\text{ox}}$. The density of defects N_{defects} is 7.2×10^{12} cm^{-2} in this example. Each O vacancy traps an electron and each broken bond traps a hole. The relaxed surface O vacancies and surface broken bonds are located on the top oxide layer which is exposed to air and the interior defects are located in the middle of the oxide layers. The atomic charges on the atoms because of the presence of defects, denoted as q(Si) for silicon atoms and q(o) for oxygen atoms, are shown in the figure. The *C-V* curves are shifted due to the defects in the oxide.

To compute the pull-in/out behavior of the switch shown in Fig. 1, we first perform a multiscale electrostatic analysis for the specified voltages to find the electrostatic force acting on the top electrode. When a voltage is applied, the potential and charge distribution in the top electrode, the dielectric oxide, and the bottom substrate can be calculated by solving Eqs. (1) and (2) self-consistently. The charge distribution on the top moveable electrode gives rise to an electrostatic force, which pulls the top electrode downward until it reaches a new position where the mechanical force f_{mech} and electrostatic force f_{elec} balance each other. When the electrostatic force exceeds the mechanical restoring force, this causes the top electrode to collapse onto the oxide layer and the corresponding voltage is the pull-in voltage. To restore the top electrode to its noncontacting or open state position, the applied voltage needs to be reduced below another critical voltage defined as the pull-out voltage. For the pull-out analysis, the self-consistent analysis is performed by gradually reducing the voltage from the pull-in voltage. When the applied voltage is less than the pull-out voltage, the equilibrium position of the top electrode is again determined from the balance of the mechanical and electrostatic forces. The difference in threshold voltages for contact actuation and release leads to a well-known condition called the pull-in/out hysteresis.[2]

For the N/MEMS switch example shown in Fig. 1, the defects in the oxide layer, where each O vacancy traps an electron and each broken bond traps a hole, are simulated.[3] To understand how these charged broken bonds and O vacancies effect the electromechanical behavior of the switch, we first compute the *C-V* characteristics of the structure by fixing the top electrode and the gap between the top electrode and the oxide. The *C-V* results are shown in Fig. 2. Positively charged defects shift the *C-V* curve to the right, and negatively charged defects shift it to the left when compared with the *C-V* curve obtained without defects. The *C-V* curve shifts to the right imply that the pull-in/out voltages are increased and shifts to the left indicate the pull-in/out voltages are decreased, as shown in Fig. 3. When nonzero atomic charges are present in the N/MEMS dielectric layer,

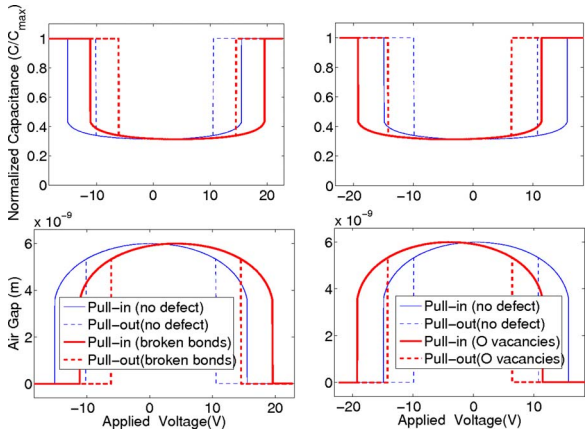

FIG. 3. (Color online) Pull-in/pull-out hysteresis of NEMS capactive switches with surface broken bonds and surface O vacancies in the oxide layers. The density of defects is 7.2×10^{12} cm^{-2}. Each broken bond traps a hole and each O vacancy traps an electron.

the pull-in/out hysteresis curve is asymmetric, i.e., the response/deflection of the top electrode to a positive applied voltage is different from the negative applied voltage. The position of the defects can also be important, i.e., defects located close to the surface of the dielectric produce larger pull-in voltage offsets compared to the defects located near the bottom electrode, as shown in Fig. 4. This is because surface defects induce a stronger electric field than the interior defects. The magnitude of the pull-in/out voltage shift increases with the density of defects. Significant shifts in the pull-in/out voltage can cause the switch to fail (e.g., switch may not open after contact) thereby creating reliability issues.

The presence of defects in practical MEMS switches can also shift the pull-in/out voltages significantly. For typical MEMS switches, quantum and surface effects may not be important in most of the regions. Hence, the pull-in/out voltage shifts can be approximately computed by the classical parallel capacitor model, which is given by $V_{\text{shift}}=(\sigma_s/\epsilon_{\text{ox}})d_{\text{ox}}=(eN_s/\epsilon_{\text{ox}})d_{\text{ox}}$, where N_s is the dielectric surface carrier density. This model has already been used to describe the drift of pull-in/out threshold voltages of capacitive MEMS switches with dielectric charges as shown in Refs. 2 and 18–20. For example, a microscale switch with a geometry of $1\times100\times45$ μm^3, $d_{\text{ox}}=0.5$ μm, and $g_0=1$ μm, is simulated. When surface broken bonds with a density of $N_{\text{defects}}=0.18\times10^{12}$ cm^{-2} is considered, $N_s=0.1805\times10^{12}$ cm^{-2} and $V_{\text{shift}}=4.439$ V are obtained by using the multiscale method. Using the classical theory, the corresponding V_{shift} is 4.408 V. Hence, for the MEMS switch considered here, the voltage shifts computed by the multiscale method and the classical method are almost equal. This example demonstrates that when quantum and surface effects are not important, the results from multiscale method and the classical method agree. However, the classical model may not be accurate at nanoscale. For example, in the case of Fig. 1, when the density of defects (surface broken bonds) N_{defects} is 1.8×10^{12} cm^{-2}, $N_s=2.251\times10^{12}$ cm^{-2}, and $V_{\text{shift}}=1.108$ V are predicted using the multiscale method. The corresponding V_{shift} is 0.641 V by the classical method. The voltage shift discrepancy between the multiscale and classical methods is because the classical model is typically not accurate for nanoscale structures, where quantum effects, surface states, and defects are important. Another disadvantage of the classical method is that N_s needs to be explicitly given and is usually not readily known. On the contrary, the multiscale method can accurately compute N_s and predict pull-in/out voltages for both MEMS and NEMS switches. The results presented above indicate that both surface and interior defects in oxide layers can have a significant effect on the pull-in and pull-out voltages of N/MEMS switches. Defects can introduce significant shifts in the C-V curves and these shifts can lead to eventual failure of the switch.

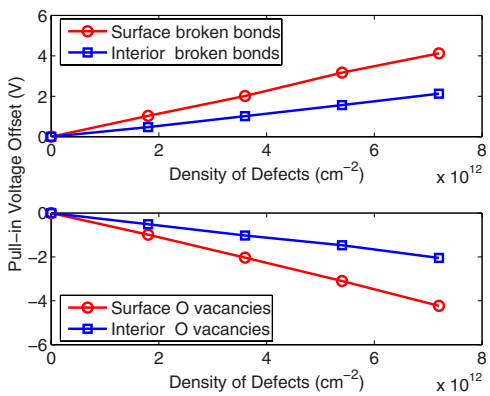

FIG. 4. (Color online) Shifts in the pull-in voltage as a function of the density of defects for surface and interior defects. The pull-in voltage offset is obtained by computing the pull-in voltage difference between with and without defects. The number of defects in the oxide layer is varied from 0, 1, 2, 3, and 4, which corresponds to the density of defects N_{defects} from 0, 1.8×10^{12}, 3.6×10^{12}, 5.4×10^{12} and 7.2×10^{12} cm^{-2}, respectively.

[1] G. M. Rebeiz, *RF MEMS: Theory, Design, and Technology* (Wiley, New Jersey, 2003).
[2] J. Wibbeler, G. Pfeifer, and M. Hietschold, Sens. Actuators, A **71**, 74 (1998).
[3] R. A. B. Devine, J.-P. Durand, and E. Dooryhee, *Structure and Imperfections in Amorphous and Crystalline Silicon Dioxide* (Wiley, NewYork, 2000).
[4] P. S. Sumant, N. R. Aluru, and A. C. Cangellaris, Int. J. RF Microwave Comput.-Aided Eng. **19**, 197 (2009).
[5] H. G. Craighead, Science **290**, 1532 (2000).
[6] J. S. Bunch, A. M. van der Zande, S. S. Verbridge, I. W. Frank, D. M. Tanenbaum, J. M. Parpia, H. G. Craighead, and P. L. McEuen, Science **315**, 490 (2007).
[7] Z. Tang, Y. Xu, G. Li, and N. R. Aluru, J. Appl. Phys. **97**, 114304 (2005).
[8] Y. Xu and N. R. Aluru, Phys. Rev. B **76**, 075304 (2007); **77**, 075313 (2008).
[9] M. Stadele, B. R. Tuttle, and K. Hess, J. Appl. Phys. **89**, 348 (2001).
[10] J. C. Slater and G. F. Koster, Phys. Rev. **94**, 1498 (1954).
[11] C. Lanczos, J. Res. Natl. Bur. Stand. **45**, 255 (1950).
[12] R. Haydock, *Recursion Method and Its Applications* (Springer, Berlin, 1985).
[13] L. Martin-Samos, Y. Limoge, and G. Roma, Phys. Rev. B **76**, 104203 (2007).
[14] J. M. Knaup, P. Deak, T. Frauenheim, A. Gali, Z. Hajnal, and W. J. Choyke, Phys. Rev. B **72**, 115323 (2005).
[15] K. Kajihara, M. Hirano, L. Skuja, and H. Hosono, Phys. Rev. B **78**, 094201 (2008).
[16] J. F. Conley, P. M. Lenahan, H. L. Evans, R. K. Lowry, and T. J. Morthorst, J. Appl. Phys. **76**, 8186 (1994).
[17] J. A. Majewski and P. Vogl, Phys. Rev. B **35**, 9666 (1987).
[18] W. M. Spengen, R. Puers, R. Mertens, and I. DeWolf, J. Micromech. Microeng. **14**, 514 (2004).
[19] S. McClure, L. D. Edmonds, R. Mihailovich, A. H. Hohnston, P. Alonzo, and J. DeNatale, IEEE Trans. Nucl. Sci. **49**, 3197 (2002).
[20] D. Molinero, R. Comulada, and L. Castaer, Appl. Phys. Lett. **89**, 103506 (2006).